

# INTERLAMINAR SHEAR REINFORCEMENT WITH ALIGNED CARBON NANOTUBE REINFORCEMENT IN COMPOSITE LAMINATES

Christopher J. Kwon<sup>1</sup>, Steven Serrano<sup>2</sup>, Carina X. Li<sup>3</sup>, Martin Levesque<sup>4</sup>, Jean-Michel Buchin<sup>5</sup>, Engin Ertem<sup>6</sup>, Alexis Ponnouradjou<sup>7</sup>, Attila Lengyel<sup>8</sup>, and Brian L. Wardle<sup>9</sup>

<sup>1</sup>Department of Aeronautics and Astronautics, Massachusetts Institute of Technology, Cambridge, MA 02139 U.S.A., Web: [aeroastro.mit.edu](http://aeroastro.mit.edu), [ckwon23@mit.edu](mailto:ckwon23@mit.edu)

<sup>2</sup>Department of Aeronautics and Astronautics, Massachusetts Institute of Technology, Cambridge, MA 02139 U.S.A., Web: [aeroastro.mit.edu](http://aeroastro.mit.edu), [serrano5@mit.edu](mailto:serrano5@mit.edu)

<sup>3</sup>Department of Aeronautics and Astronautics, Massachusetts Institute of Technology, Cambridge, MA 02139 U.S.A., Web: [aeroastro.mit.edu](http://aeroastro.mit.edu), [carinali@mit.edu](mailto:carinali@mit.edu)

<sup>4</sup>Hutchinson Aéronautique & Industrie, 3650 du Tricentenaire Blvd., H1B 5M8, Montréal, QC, Canada, Web: [www.hutchinson.com](http://www.hutchinson.com), [martin.levesque@hutchinson.com](mailto:martin.levesque@hutchinson.com)

<sup>5</sup>Hutchinson SA, Rue Gustave Nourry BP 31, 45120 Chalette-Sur-Loing, France, Web: [www.hutchinson.com](http://www.hutchinson.com), [jean-michel.buchin@hutchinson.com](mailto:jean-michel.buchin@hutchinson.com)

<sup>6</sup>Hutchinson SA, Rue Gustave Nourry BP 31, 45120 Chalette-Sur-Loing, France, Web: [www.hutchinson.com](http://www.hutchinson.com), [engin.ertem@hutchinson.com](mailto:engin.ertem@hutchinson.com)

<sup>7</sup>Hutchinson SA, Rue Gustave Nourry BP 31, 45120 Chalette-Sur-Loing, France, Web: [www.hutchinson.com](http://www.hutchinson.com), [alexis.ponnouradjou@hutchinson.com](mailto:alexis.ponnouradjou@hutchinson.com)

<sup>8</sup>Mide Technology | A Hutchinson Company, 475 Wildwood Ave, Woburn, MA 01801 U.S.A., Web: [www.mide.com](http://www.mide.com), [alengyel@hutchinsoninc.com](mailto:alengyel@hutchinsoninc.com)

<sup>9</sup>Department of Aeronautics and Astronautics, Massachusetts Institute of Technology, Cambridge, MA 02139 U.S.A., Department of Mechanical Engineering, Massachusetts Institute of Technology, Cambridge, MA 02139 U.S.A., Web: [meche.mit.edu](http://meche.mit.edu), [wardle@mit.edu](mailto:wardle@mit.edu)

**Keywords:** *Carbon nanotubes, Short beam shear, Nano-engineered, Mechanical properties*

## ABSTRACT

Aerospace-grade, quasi-isotropic carbon fiber laminates are reinforced at the through-thickness interlaminar interfaces with high densities of aligned carbon nanotubes to realize a nano-engineered hierarchical carbon fiber reinforced polymer (CFRP) laminated architecture. Such materials have improved interlaminar and intralaminar properties with increased interlaminar fracture toughness, substructural in-plane strengths, and high cycle fatigue life. The interlaminar shear strength of the reinforced laminates is examined using short beam shear testing compared to the baseline system. The short beam shear testing demonstrated no statistically significant increase in static SBS strength, which is linked to the complex stress state and potential coupling of various failure mechanisms that have been found to mask the structural improvement of the nano-reinforcement. These findings agree with previous literature that used similar quasi-isotropic, unidirectional CFRP material systems and the same laminate layup manufacturing processes.

## 1 INTRODUCTION

Fiber-reinforced polymer composite materials, such as carbon fiber-reinforced plastics (CFRP) and glass fiber-reinforced plastics (GFRP), have emerged as high-performance materials that provide sundry advantages such as their high strength-to-weight ratio, fatigue resistance, and stiffness [1]. These material properties have catalyzed their widespread adoption in various industries - such as aerospace, biomedical, and automotive - where these materials have supplemented and eclipsed their metal counterparts in producing advanced, load-bearing structures. However, despite their many advantageous properties, a fundamental constraint to these composite materials is their relatively weak mechanical strength at the resin-rich region between the fiber-reinforced ply layers [2]. This limitation causes these

materials to be particularly susceptible to delamination and related failure modes when subjected to specific loading conditions, which pose severe consequences for the structural performance reliability of composite structures.

To mitigate such effects, various methodologies have emerged to mechanically reinforce the interlaminar regions, including stitching, z-pinning, and 3D weaving [3–9]. However, these reinforcement materials are large in relation to the composite’s microfibers which can pose issues in manufacturing that significantly decrease the in-plane mechanical properties of the laminate [3]. With growing interest in nanomaterials in recent years, other methodologies have emerged that explore implementing such materials as reinforcement mechanisms [10].

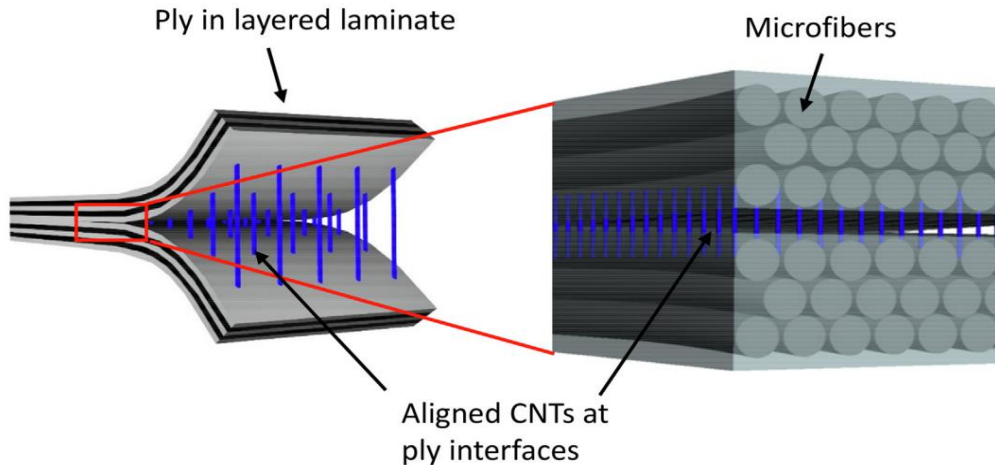


Figure 1. Conceptual illustration of hierarchical nano-engineered composite architecture with the placement of aligned carbon nanotubes at the nanostitched laminate interface [11].

One of the primary benefits of these reinforcements, in particular carbon nanotubes (CNTs), is that they are comparably smaller than microfibers and possess excellent material properties that are comparable to or exceed those of carbon-derived microfibers, which effectively reinforces the laminate without deteriorating the in-plane properties [1,12,13]. In addition, CNTs also possess outstanding electrical [14–16] and thermal properties [14,15,17–19] which can enable composite structures to have multifunctional qualities [20–22]. Introduced by Garcia et al., aligned carbon nanotubes (A-CNTS) that are transferred onto the through-thickness interlaminar regions of the composite exhibit a nanoscale stitching effect that introduces energy dissipating mechanisms that delay the initiation and propagation of delamination (see Figure 1) [23]. This nano-reinforcement method, termed “nanostitch”, has been shown to improve both intralaminar and interlaminar properties with 2.5-3X enhancement in mode I and mode II fracture toughness [23,24], 14-40% increase in substructural in-plane strengths [25], and 249% improvement for high-cycle fatigue (with 60% of static SBS strength load level) [11].

This study explored the structural improvements of A-CNT nanostitched quasi-isotropic symmetric CFRP laminates using short beam shear (SBS) testing. Nanostitched CFRP specimens are compared to a baseline CFRP laminate without CNT reinforcement. The effect of CNT reinforcement in the laminate is visualized using optical microscopy, micro-computed tomography ( $\mu$ CT), and scanning electron microscopy (SEM). This study aims to observe the structural improvement and elucidate the mechanisms of nanostitching in fiber-reinforced laminated structures.

## 2 METHODS

Methodologies for synthesizing the A-CNTs are first presented. Then, fabrication of the baseline and nanostitched composite laminates, including transfer of the A-CNTs to the microfiber plies, and characterization are followed. Finally, guidelines for short beam shear testing are outlined.

## 2.1 A-CNT Synthesis

The A-CNTs were grown on 3 cm x 8 cm SiO<sub>2</sub>/Si substrates in a 44 mm inner diameter quartz tube furnace (Lindbergh/BlueM) via chemical vapor deposition (CVD). This synthesis process utilizes thermal catalytic CVD, set at atmospheric pressure and 680 °C, using ethylene as the carbon source and 600 ppm of water vapor added to inert helium gas [26]. The water aids in reducing the bond at the CNT-substrate interface to facilitate the transfer of the CNTs onto the plies. A 1nm Fe and 10nm Al<sub>2</sub>O<sub>3</sub> catalytic layer were deposited onto the SiO<sub>2</sub>/Si substrates via an electron beam physical vapor deposition instrument (Temascal FC-2800). The growth time was 35 seconds to produce 20±4 μm CNT forests. The CNTs exhibit an average outer diameter of ~8 nm (3-7 walls with an inner diameter of ~5 nm and intrinsic CNT density of ~1.6 g/cm<sup>3</sup>) [27], inter-CNT spacing of ~60 nm [28], and volume fraction of ~1% CNTs [27]. The height of the CNTs on the substrates was obtained by measuring the difference in z-axis travel between the substrate's focal planes and the top of the CNT forest in a light optical microscope at 20X magnification. The heights were measured at the four corners near the substrate edges along the substrate length (8 cm) direction. The forest height was taken as the average of the four measurements. This method has a resolution of ±2 μm.

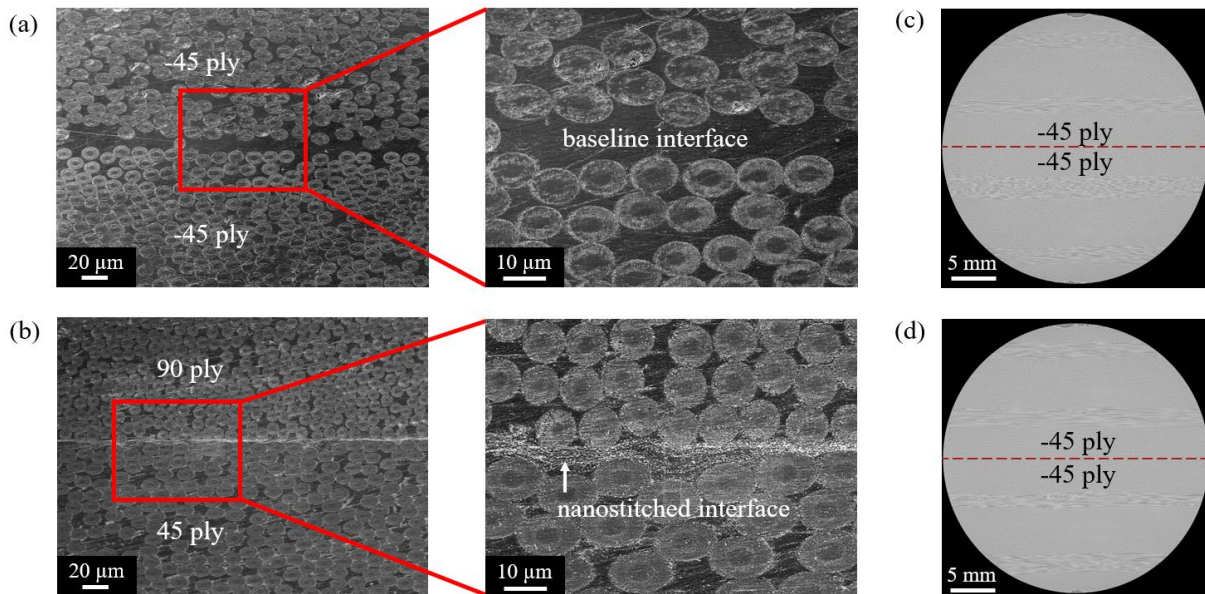


Figure 2. Representative SEM images of the interlaminar region at the (a) -45/-45 interface for baseline specimen and at the (b) 90/45 interface A-CNT reinforced specimen. Representative ply-wise μ-CT images at the spanwise midline for (c) baseline and (d) nanostitched specimens.

## 2.2 Laminate Fabrication And Characterization

The laminate utilizes a 16-ply quasi-isotropic layup ((0/90/±45)<sub>2</sub>)<sub>s</sub> using Hexel AS4/8552 UD prepreg with a ply thickness of 0.182 mm. Both the nanostitched specimens and baseline specimens were generated from a single laminate. The nanostitched specimens feature 15 through-thickness interfaces with A-CNT reinforcement. The A-CNT transfer is over 95% effective based on the surface area. The CNT-grown substrates are manually transferred onto the prepreg surface using procedures outlined in previous work [29–31]. A guaranteed non-porous Teflon (GNPT) stencil of the same dimension as the laminate plies was created with a 3 cm x 8 cm cut-out specifying the location of the nanostitched specimens. The CNT-grown substrate was positioned about the cut-out on the GNPT stencil and applied to the ply with the CNT side in contact with the ply face. While maintaining contact on the substrate, gentle pressure was applied for several seconds for all the A-CNTs to effectively adhere to the ply surface from which the substrate can be easily removed and the proceeding ply is laid. This transfer process was repeated for each interlaminar interface until the entire stack-up was complete.

The laminate was cured in an autoclave (ARC Technologies LLC, Amesbury, MA) following the manufacturer specifications: apply full vacuum and 15 psig pressure, heat at 3-5 °F/min to 225 °F, hold at 225 °F for 30-60 minutes, raise pressure to 85-100 psig, vent vacuum when pressure reaches 30 psig, hold at 350 °F for 120±10 min, and cool at 2-5 °F/min to 150 °F and vent pressure. Specimens were cut and polished to SBS coupon size following ASTM D2344 [32]. Representative scanning electron microscopy (SEM) in Figure 2 shows that A-CNTs permeate the ply-to-ply interfaces in nanostitched specimens in contrast to the resin-rich ply-to-ply interfaces in the baseline specimens. Furthermore, introducing A-CNTs does not exhibit a notable increase in interlaminar thickness. The  $\mu$ -CT images in Figure 2 show that the specimens have 0.00% void content. The baseline and nanostitched specimens have a thickness of 2.91±0.04 mm and 2.93±0.03 mm, respectively, indicating that nanostitch does not notably increase the interlaminar thickness, consistent with previous studies that followed the same procedures [25]. The interlaminar thickness was measured at 27 equally spaced locations and averaged for in representative optical micrographs (see Figure 3.b, c). The averaged interlaminar thickness of the baseline and nanostitched specimens is 9.37±0.62  $\mu$ m and 10.185±0.66  $\mu$ m, respectively, which shows that there is no statistically significant difference in the interlaminar thickness. Consequently, the overall laminate microfiber volume fraction and other attributes were maintained.

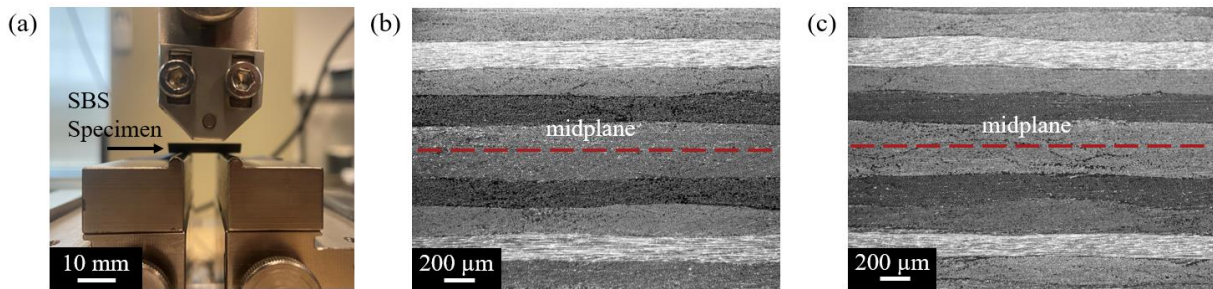


Figure 3. Short beam shear (SBS) load rig and laminate cross sections: (a) SBS test optical image. Representative optical darkfield micrographs about the midplane in the ply-wise direction for (b) baseline and (c) nanostitched specimens.

### 2.3 Short Beam Shear Testing

ASTM D2344 [32] outlines the dimensions for an SBS coupon: (a) the minimum length-to-thickness ratio of the coupon is 4, (b) the minimum thickness of the coupon is 2 mm, (c) the length of the coupon should be 6X the thickness, (d) the width of the coupon should be 2X the thickness, (e) the coupon should be balanced and symmetric, (f) at least 10% of the coupon's plies are 0° plies to the spanwise direction. With a thickness of ~3 mm, specimens were manufactured to have a width of 6 mm and a length of 18 mm. A 3-point bending load, as shown in Figure 3.a, was used to test the specimens. This test was conducted on a Zwick/Rowell Z010 mechanical tester with a 10 kN load cell in displacement control. Each specimen was continuously loaded at 1 mm/min until one of the following stop criteria occurred: (a) a 30% load drop off, (b) the head travel exceeds the specimen thickness, (c) the specimen failed and split into two pieces. The displacement and load were recorded every 250 ms, and the static SBS strength was determined using the following:

$$\sigma_{SBS} = 0.75 \times \frac{P_{max}}{w \times t} \quad (1)$$

$P_{max}$  is the maximum measured load, and  $w$  and  $t$  are the specimen's width and thickness. All the samples are inspected under an optical microscope to assess crack propagation behaviors and their locations.

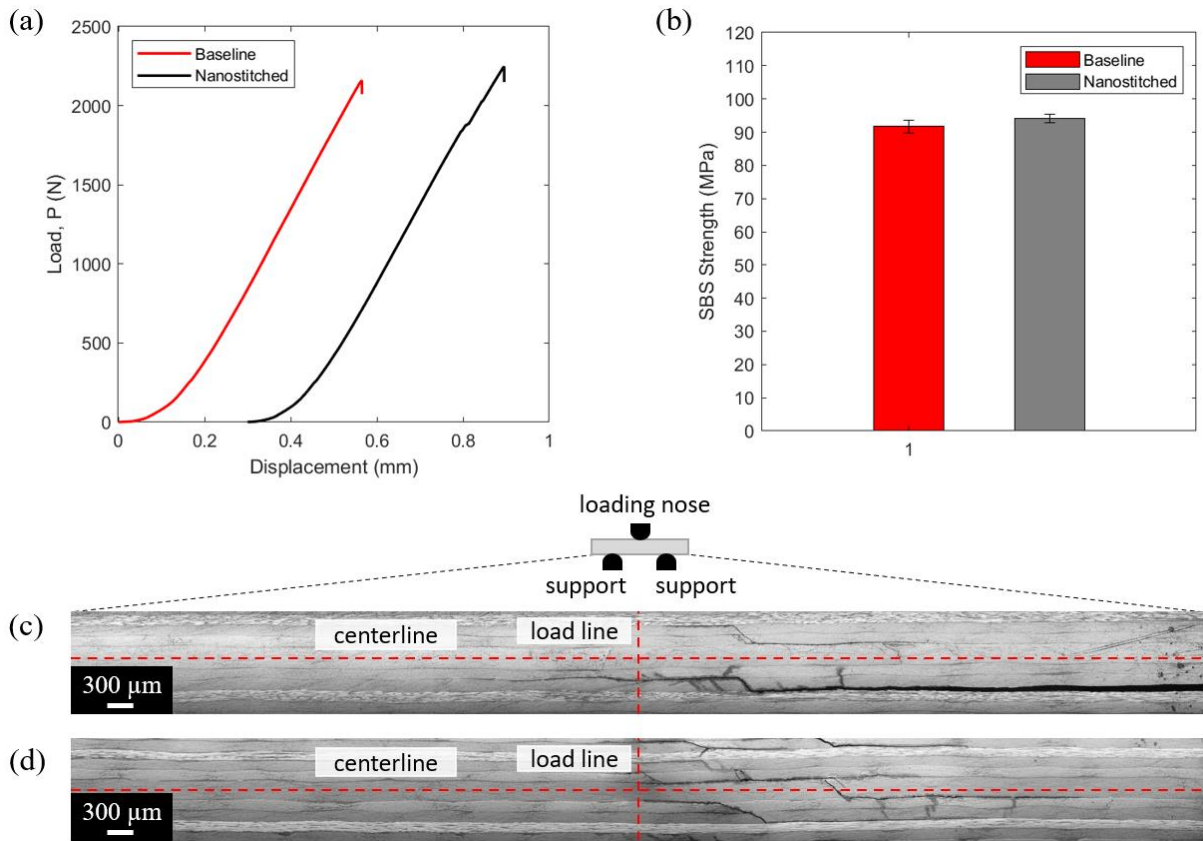


Figure 4. Short beam shear testing results: (a) representative load vs. displacement curves for baseline and nanostitched specimens. For comparison, the curves were shifted along the x-axis by 0.3 mm. (b) SBS strength comparison between the baseline and nanostitched specimen with standard error bars.

Representative panoramic postmortem optical micrographs for (c) baseline and (d) nanostitched specimens detailing crack propagation behavior with a coupling of delamination, intralaminar crack deflections, and microfiber breakage. The panoramic effect is achieved by stitching a series of smaller optical micrographs using Adobe Lightroom.

### 3 RESULTS AND DISCUSSION

The test specimens failed in a brittle fashion with the load criterion of a load drop of 30% rather than the other stop criterion of two-piece specimen split failure or head travel deflection limit. As identified in ASTM D2344 [32], typical failure modes include delamination at the midline about the specimen's cross-section, delamination at the free edges along or near the midline, microfiber breaks, and compressive damage at the regions of applied load about the surface of the specimen. Representative load-displacement curves for the baseline and nanostitched specimens are shown in Figure 4.a. As shown in Figure 4.b, the baseline specimens and nanostitched specimens are shown to exhibit an SBS strength of  $91.7 \pm 1.85$  MPa and  $94.1 \pm 1.25$  MPa, respectively.

The results from the testing type show that there is no statistically significant difference between baseline and nanostitched specimens for static SBS strength. This agrees with prior work [11] that used the also used Hexcel AS4/8552 UD prepreg, although thinner at  $\sim 130$   $\mu\text{m}$  ply thickness, with a quasi-isotropic layup  $[(0_3/90_{\pm 45})_2]_s$ , and another study [33] that used a different UD material system (Toho Tenax HTS40/Q-1112) with a quasi-isotropic layup  $[(0_3/90_3/\pm 45_3)_2]_s$ . An SBS strength sensitivity analysis using a finite element model [11] also agrees with the experimental conclusion of no statistically significant difference. This contrasts with other work that has shown an  $>8\%$  statistically significant increase in SBS strength of a different UD material system (IM7/8552) of the same layup procedure [31]. Small, negligible increases in static SBS strength are shown in the SBS testing across the different

material systems. However, nanostitch has largely increased fatigue life and other strength tests such as open-hole compression and filled-hole tension (tension-bearing) [11, 25].

The stress distribution has been noted to have a complex profile in the laminated composite under SBS loading [11]. In addition, significant compressive stresses are also locally present in zones with high shear stress concentrations, affecting interlaminar shear failure mechanisms. Thus, even if a stronger and more robust interface from A-CNT reinforcement is produced, the strength increases of such structures may be masked in the SBS test, with the ultimate failure load being dictated by complex and likely coupled failure mechanisms [11]. Representative panoramic, postmortem optical micrographs (see Figure 4.c,d) for both the baseline and nanostitched specimens demonstrate no notably significant difference in damage modes.

#### 4 CONCLUSION

A nano-engineered hierarchical composite architecture was developed by implementing through-thickness aligned carbon nanotube reinforcements at the ply-to-ply interfaces of aerospace-grade UD CFRP materials. The A-CNTs can easily be transferred to the ply-to-ply interfaces using existing layup manufacturing procedures without affecting the overall laminate thickness and damaging the ply microfibers. The reinforced laminate's mechanical performance compared to a baseline laminate for short beam shear strength testing was examined. No static SBS strength improvement of the reinforced laminate was observed, consistent with prior work for the same material system at smaller ply thicknesses (gsm of prepreg).

#### ACKNOWLEDGEMENTS

This work is supported by Hutchinson. This work used facilities supported in part by the U. S. Army Research Laboratory and the U. S. Army Research Office through the Institute for Soldier Nanotechnologies, under contract number W911NF-13-D-0001, and it was carried out in part through the use of MIT.nano's facilities.

#### REFERENCES

- [1] Gorbatikh, L., Wardle, B. L., and Lomov, S. V. "Hierarchical Lightweight Composite Materials for Structural Applications." *MRS Bulletin*, Vol. 41, No. 09, 2016, pp. 672–677. <https://doi.org/10.1557/mrs.2016.170>.
- [2] Faggiani, A., and Falzon, B. G. "Predicting Low-Velocity Impact Damage on a Stiffened Composite Panel." *Composites Part A: Applied Science and Manufacturing*, Vol. 41, No. 6, 2010, pp. 737–749. <https://doi.org/10.1016/j.compositesa.2010.02.005>.
- [3] Tong, L., Mouritz, A. P., and Bannister, M. *3D Fibre Reinforced Polymer Composites*. Elsevier, 2002.
- [4] Dransfield, K. A., Jain, L. K., and Mai, Y.-W. "On the Effects of Stitching in CFRPs—I. Mode I Delamination Toughness." *Composites Science and Technology*, Vol. 58, No. 6, 1998, pp. 815–827. [https://doi.org/10.1016/S0266-3538\(97\)00229-7](https://doi.org/10.1016/S0266-3538(97)00229-7).
- [5] Mouritz, A. P., Leong, K. H., and Herszberg, I. "A Review of the Effect of Stitching on the In-Plane Mechanical Properties of Fibre-Reinforced Polymer Composites." *Composites Part A: Applied Science and Manufacturing*, Vol. 28, No. 12, 1997, pp. 979–991. [https://doi.org/10.1016/S1359-835X\(97\)00057-2](https://doi.org/10.1016/S1359-835X(97)00057-2).
- [6] Larsson, F. "Damage Tolerance of a Stitched Carbon/Epoxy Laminate." *Composites Part A: Applied Science and Manufacturing*, Vol. 28, No. 11, 1997, pp. 923–934. [https://doi.org/10.1016/S1359-835X\(97\)00063-8](https://doi.org/10.1016/S1359-835X(97)00063-8).
- [7] Partridge, I. K., and Cartié, D. D. R. "Delamination Resistant Laminates by Z-Fiber® Pinning: Part I Manufacture and Fracture Performance." *Composites Part A: Applied Science and Manufacturing*, Vol. 36, No. 1, 2005, pp. 55–64. <https://doi.org/10.1016/j.compositesa.2004.06.029>.
- [8] Tan, K. T., Yoshimura, A., Watanabe, N., Iwahori, Y., and Ishikawa, T. "Effect of Stitch Density and Stitch Thread Thickness on Damage Progression and Failure Characteristics of Stitched

- Composites under Out-of-Plane Loading.” *Composites Science and Technology*, Vol. 74, 2013, pp. 194–204. <https://doi.org/10.1016/j.compscitech.2012.11.001>.
- [9] Aymerich, F. “Effect of Stitching on the Static and Fatigue Performance of Co-Cured Composite Single-Lap Joints.” *Journal of Composite Materials*, Vol. 38, No. 3, 2004, pp. 243–257. <https://doi.org/10.1177/0021998304039271>.
- [10] Wardle, B. L., Koo, J. H., Odegard, G. M., and Seidel, G. D. “Advanced Nano-engineered Materials.” p. 30.
- [11] Ni, X., Furtado, C., Kalfon-Cohen, E., Zhou, Y., Valdes, G. A., Hank, T. J., Camanho, P. P., and Wardle, B. L. “Static and Fatigue Interlaminar Shear Reinforcement in Aligned Carbon Nanotube-Reinforced Hierarchical Advanced Composites.” *Composites Part A: Applied Science and Manufacturing*, Vol. 120, 2019, pp. 106–115. <https://doi.org/10.1016/j.compositesa.2019.02.023>.
- [12] De Volder, M. F. L., Tawfick, S. H., Baughman, R. H., and Hart, A. J. “Carbon Nanotubes: Present and Future Commercial Applications.” *Science*, Vol. 339, No. 6119, 2013, pp. 535–539. <https://doi.org/10.1126/science.1222453>.
- [13] Naskar, A. K., Keum, J. K., and Boeman, R. G. “Polymer Matrix Nanocomposites for Automotive Structural Components.” *Nature Nanotechnology*, Vol. 11, No. 12, 2016, pp. 1026–1030. <https://doi.org/10.1038/nnano.2016.262>.
- [14] Marconnet, A. M., Panzer, M. A., and Goodson, K. E. “Thermal Conduction Phenomena in Carbon Nanotubes and Related Nanostructured Materials.” *Reviews of Modern Physics*, Vol. 85, No. 3, 2013, pp. 1295–1326. <https://doi.org/10.1103/RevModPhys.85.1295>.
- [15] Meunier, V., Souza Filho, A. G., Barros, E. B., and Dresselhaus, M. S. “Physical Properties of Low-Dimensional  $\text{sp}^2$ -Based Carbon Nanostructures.” *Reviews of Modern Physics*, Vol. 88, No. 2, 2016, p. 025005. <https://doi.org/10.1103/RevModPhys.88.025005>.
- [16] Ebbesen, T. W., Lezec, H. J., Hiura, H., Bennett, J. W., Ghaemi, H. F., and Thio, T. “Electrical Conductivity of Individual Carbon Nanotubes.” *Nature*, Vol. 382, No. 6586, 1996, pp. 54–56. <https://doi.org/10.1038/382054a0>.
- [17] Che, J., Çagin, T., and III, W. A. G. “Thermal Conductivity of Carbon Nanotubes.” *Nanotechnology*, Vol. 11, No. 2, 2000, p. 65. <https://doi.org/10.1088/0957-4484/11/2/305>.
- [18] Gojny, F. H., Wichmann, M. H. G., Fiedler, B., and Schulte, K. “Influence of Different Carbon Nanotubes on the Mechanical Properties of Epoxy Matrix Composites – A Comparative Study.” *Composites Science and Technology*, Vol. 65, No. 15, 2005, pp. 2300–2313. <https://doi.org/10.1016/j.compscitech.2005.04.021>.
- [19] Dresselhaus, M. S., Dresselhaus, G., Eklund, P. C., and Rao, A. M. Carbon Nanotubes. In *The Physics of Fullerene-Based and Fullerene-Related Materials* (W. Andreoni, ed.), Springer Netherlands, Dordrecht, 2000, pp. 331–379.
- [20] Coleman, J. N., Khan, U., Blau, W. J., and Gun’ko, Y. K. “Small but Strong: A Review of the Mechanical Properties of Carbon Nanotube–Polymer Composites.” *Carbon*, Vol. 44, No. 9, 2006, pp. 1624–1652. <https://doi.org/10.1016/j.carbon.2006.02.038>.
- [21] Gibson, R. F. “A Review of Recent Research on Mechanics of Multifunctional Composite Materials and Structures.” *Composite Structures*, Vol. 92, No. 12, 2010, pp. 2793–2810. <https://doi.org/10.1016/j.compstruct.2010.05.003>.
- [22] Gao, L., Chou, T.-W., Thostenson, E. T., Zhang, Z., and Coulaud, M. “In Situ Sensing of Impact Damage in Epoxy/Glass Fiber Composites Using Percolating Carbon Nanotube Networks.” *Carbon*, Vol. 49, No. 10, 2011, pp. 3382–3385. <https://doi.org/10.1016/j.carbon.2011.04.003>.
- [23] Garcia, E., Wardle, B., and John Hart. “Joining Prepreg Composite Interfaces with Aligned Carbon Nanotubes - ScienceDirect.” *Composites Part A: Applied Science and Manufacturing*, Vol. 39, No. 6, 2008, pp. 1065–1070. <https://doi.org/10.1016/j.compositesa.2008.03.011>.
- [24] Falzon, B. G., Hawkins, S. C., Huynh, C. P., Radjef, R., and Brown, C. “An Investigation of Mode I and Mode II Fracture Toughness Enhancement Using Aligned Carbon Nanotubes Forests at the Crack Interface.” *Composite Structures*, Vol. 106, 2013, pp. 65–73. <https://doi.org/10.1016/j.compstruct.2013.05.051>.
- [25] Guzman de Villoria, R., Hallander, P., Ydrefors, L., Nordin, P., and Wardle, B. L. “In-Plane Strength Enhancement of Laminated Composites via Aligned Carbon Nanotube Interlaminar

- Reinforcement.” *Composites Science and Technology*, Vol. 133, 2016, pp. 33–39. <https://doi.org/10.1016/j.compscitech.2016.07.006>.
- [26] Stein, I. Y., Kaiser, A. L., Constable, A. J., Acauan, L., and Wardle, B. L. “Mesoscale Evolution of Non-Graphitizing Pyrolytic Carbon in Aligned Carbon Nanotube Carbon Matrix Nanocomposites.” *Journal of Materials Science*, Vol. 52, No. 24, 2017, pp. 13799–13811. <https://doi.org/10.1007/s10853-017-1468-9>.
- [27] Lee, J., Stein, I. Y., Devoe, M. E., Lewis, D. J., Lachman, N., Kessler, S. S., Buschhorn, S. T., and Wardle, B. L. “Impact of Carbon Nanotube Length on Electron Transport in Aligned Carbon Nanotube Networks.” *Applied Physics Letters*, Vol. 106, No. 5, 2015, p. 053110. <https://doi.org/10.1063/1.4907608>.
- [28] Stein, I. Y., and Wardle, B. L. “Coordination Number Model to Quantify Packing Morphology of Aligned Nanowire Arrays.” *Physical Chemistry Chemical Physics*, Vol. 15, No. 11, 2013, p. 4033. <https://doi.org/10.1039/c3cp43762k>.
- [29] Wardle, B. L., Saito, D. S., García, E. J., Hart, A. J., de Villoria, R. G., and Verploegen, E. A. “Fabrication and Characterization of Ultrahigh-Volume-Fraction Aligned Carbon Nanotube–Polymer Composites.” *Advanced Materials*, Vol. 20, No. 14, 2008, pp. 2707–2714. <https://doi.org/10.1002/adma.200800295>.
- [30] Hart, A. J., and Slocum, A. H. “Rapid Growth and Flow-Mediated Nucleation of Millimeter-Scale Aligned Carbon Nanotube Structures from a Thin-Film Catalyst.” *The Journal of Physical Chemistry B*, Vol. 110, No. 16, 2006, pp. 8250–8257. <https://doi.org/10.1021/jp055498b>.
- [31] Lewis, D., and Wardle, B. L. Interlaminar Shear Strength Investigation of Aligned Carbon Nanotube-Reinforced Prepreg Composite Interfaces. In *56th AIAA/ASCE/AHS/ASC Structures, Structural Dynamics, and Materials Conference*, American Institute of Aeronautics and Astronautics, 2015.
- [32] Conshohocken, W. ASTM D 2344/D 2344M-16, Standard Test Method for Short-Beam Strength of Polymer Matrix Composite Materials and Their Laminates. PA: ASTM International, Sep 03, 2022.
- [33] Kalfon-Cohen, E., Kopp, R., Furtado, C., Ni, X., Arteiro, A., Borstnar, G., Mavrogordato, M. N., Sinclair, I., Spearing, S. M., Camanho, P. P., and Wardle, B. L. “Synergetic Effects of Thin Plies and Aligned Carbon Nanotube Interlaminar Reinforcement in Composite Laminates.” *Composites Science and Technology*, Vol. 166, 2018, pp. 160–168. <https://doi.org/10.1016/j.compscitech.2018.01.007>.